Biochimica et Biophysica Acta 1840 (2014) 170–183

Contents lists available at ScienceDirect

Biochimica et Biophysica Acta

journal homepage: www.elsevier.com/locate/bbagen

Structure–function relationships of the peptide Paulistine: A novel toxin from the venom of the social wasp *Polybia paulista*

Paulo Cesar Gomes [a], Bibiana Monson de Souza [a], Nathalia Baptista Dias [a], Patrícia Brigatte [b], Danilo Mourelle [a], Helen Andrade Arcuri [b], Marcia Perez dos Santos Cabrera [c], Rodrigo Guerino Stabeli [b], João Ruggiero Neto [c], Mario Sergio Palma [a,*]

[a] Department of Biology/CEIS/LSBZ, Institute of Biosciences, São Paulo State University (UNESP), Rio Claro, SP, Brazil
[b] Fundação Oswaldo Cruz, MS/Fiocruz Rondônia, Porto Velho, RO, Brazil
[c] Department of Physics/IBILCE, São Paulo State University (UNESP), São José do Rio Prêto, SP, Brazil

ARTICLE INFO

Article history:
Received 4 June 2013
Received in revised form 20 August 2013
Accepted 27 August 2013
Available online 2 September 2013

Keywords:
Wasp venom
Molecular structure
Disulphide bridge
Pain
Hyperalgesia
Inflammation

ABSTRACT

Background: The peptide Paulistine was isolated from the venom of wasp *Polybia paulista*. This peptide exists under a natural equilibrium between the forms: oxidised — with an intra-molecular disulphide bridge; and reduced — in which the thiol groups of the cysteine residues do not form the disulphide bridge. The biological activities of both forms of the peptide are unknown up to now.
Methods: Both forms of Paulistine were synthesised and the thiol groups of the reduced form were protected with the acetamidemethyl group [Acm-Paulistine] to prevent re-oxidation. The structure/activity relationships of the two forms were investigated, taking into account the importance of the disulphide bridge.
Results: Paulistine has a more compact structure, while Acm-Paulistine has a more expanded conformation. Bioassays reported that Paulistine caused hyperalgesia by interacting with the receptors of lipid mediators involved in the cyclooxygenase type II pathway, while Acm-Paullistine also caused hyperalgesia, but mediated by receptors involved in the participation of prostanoids in the cyclooxygenase type II pathway.
Conclusion: The acetamidemethylation of the thiol groups of cysteine residues caused small structural changes, which in turn may have affected some physicochemical properties of the Paulistine. Thus, the dissociation of the hyperalgesy from the edematogenic effect when the actions of Paulistine and Acm-Paulistine are compared to each other may be resulting from the influence of the introduction of Acm-group in the structure of Paulistine.
General significance: The peptides Paulistine and Acm-Paulistine may be used as interesting tools to investigate the mechanisms of pain and inflammation in future studies.

1. Introduction

The venoms of the social Hymenoptera insects are used as part of their chemical weaponry for defence and/or prevention against infection by pathogenic microorganisms; venom components may act as toxins, hormones, antibiotics, and defensins, interacting with different pharmacological targets and causing pain, inflammation, changes in blood pressure, cardiac arrhythmia, and neurotoxicity amongst other toxic effects [1–3].

Wasp venoms are composed of a complex mixture of free amino acids, biogenic amines, and a series of polycationic peptides and proteins [4]. The peptides represent approximately 70% of the dry weight of venoms from social wasps [5]. Most of these peptides are linear, polycationic and amphipathic molecules with a high α-helix content in their secondary structures. These peptides generally cause cell lysis, hemolysis, antibiosis, smooth muscle contraction, and chemotaxis. Venom peptides may also promote the release of activators/mediators from mast cells, leukocytes, and platelets through their interaction with G-protein coupled receptors on the plasma membranes of these cells [3].

Identification of the peptides in venoms is important to characterise the pharmacological symptoms observed during the envenoming process. This knowledge will help physicians to assist the victims of stinging incidents. The pharmacological properties of wasp venoms have not yet been fully investigated because of the limited amount of venom produced by wasps and the low abundance of each natural peptide in these venoms.

The peptides from the venoms of social wasps are generally classified into families according to the type of biological activities exhibited by these peptides: i) mastoparans, which cause degranulation of mast cells; ii) chemotactic peptides, which promote chemotaxis of polymorphonucleated leukocytes [6]; iii) wasp kinins, which are known to be pain-inducing peptides; and iv) very short peptides, possessing a series of inflammatory activities [7].

A novel peptide named Paulistine with an unusual structure amongst the peptide toxins from social wasps was isolated from the venom of the wasp *Polybia paulista*, this peptide has 21 amino acid residues in its sequence with a single intramolecular disulphide bridge.

* Corresponding author. Tel.: +55 19 35264163; fax: +55 19 35348523.

0304-4165/$ – see front matter © 2013 Elsevier B.V. All rights reserved.
http://dx.doi.org/10.1016/j.bbagen.2013.08.024

Intramolecular disulphide bridges have already been reported for some honeybee venom peptides, such as Apamine, Tertiapine, and MCD-Peptide, which possess four cysteine residues forming two intramolecular disulphide bridges [8]. A peptide similar to Paulistine named Sylverine was previously reported by Dohtsu et al. (1993) [9] in the venom from the neotropical social wasp *Protonectarina sylveirae*; however, the structure and biological activities of this peptide were never investigated. Thus, the objective of the present study was to characterise the structure/function relationship of the novel wasp venom peptide Paulistine, taking into account the importance of the oxidised and reduced forms of the disulphide bridge for the maintenance of both the molecular structure and the biological activities of this peptide.

2. Material and methods

2.1. Biological material

The social wasp *P. paulista* was collected in Rio Claro, SP, southeast Brazil (S22°23′49.7″; W047°32′54″), and immediately frozen and stored at −20 °C. The venom reservoirs of 500 wasps (5 mg venom) were removed with forceps and microscissors and suspended in 50% (v/v) acetonitrile (MeCN). The reservoirs were then perforated with a sharp metallic stylet, and the venom was extracted by washing the biological material three times with the solvent. The suspension was then centrifuged at 10,000 ×*g* for 10 min at 4 °C. The supernatants were collected, pooled, lyophilised, and stored at −80 °C until use.

2.2. Venom fractionation

The venom extract from *P. paulista* was chromatographed in a Capcell Pack C-18 UG120 column (10 mm × 250 mm, 5 μm, Shisheido) under a linear gradient from 5 to 60% (v/v) MeCN/H_2O [containing 0.1% (v/v) trifluoroacetic acid (TFA)] at a flow rate of 2.0 mL/min over 60 min and monitored by UV absorption at 214 nm with a UV-DAD detector (Shimadzu, mod. SPD-M10A). The fractions were manually collected in glass vials and dried using a lyophiliser. Fraction 10 (containing both the oxidised and reduced forms of Paulistine) was re-fractionated by reverse-phase HPLC with a C-18 (ODS) Capcell Pack UG120 column (10 mm × 250 mm, 5 μm, Shisheido) under an isocratic condition with 40% (v/v) MeCN/H_2O (containing 0.1%TFA) at a flow rate of 2.0 mL/min over 20 min. The elution was monitored by measurement of the UV absorption at UV 214 nm.

2.3. Amino acid sequencing

The amino acids were sequenced using a gas phase sequencer PPSQ-21A (Shimadzu) based on automated Edman degradation chemistry.

2.4. Mass spectrometry

Mass spectrometric analysis was performed in an Ion Trap-Time of Flight hybrid mass spectrometer (LCMS-IT-TOF) produced by Shimadzu Co. The samples were injected into the LC–MS system with an autosampler injector at a flow rate of 0.2 mL/min of MeCN 50% (v/v). All analyses were performed in the positive electrospray ionisation (ESI+) mode using typical conditions: CDL temperature of 200 °C, a capillary voltage of 4.5 kV, a cone voltage of 3.5 V, a flow rate of nebuliser gas (nitrogen) of approximately 1.5 L/h and a drying gas (nitrogen) flow rate of 100 L/h. The ESI mass spectra were obtained in the continuous acquisition mode, scanning from m/z 50 to 4000 during 2 min. The data were acquired and analysed using LCMS solution software (SHIMADZU).

2.5. Peptide synthesis

The peptides were prepared by stepwise manual solid-phase synthesis using N-9-fluorophenylmethoxy-carbonyl (Fmoc) chemistry with Novasyn TGS resin (NOVABIOCHEM). Side-chain protective groups included trityl (Trt) for glutamine, t-butyl (tBu) for serine and threonine, t-butoxycarbonyl (Boc) for lysine, and β-t-butyl ester (OtBu) for aspartic acid. The side-chain protective group trityl (Trt) was used in the synthesis of the oxidised peptide (with the disulphide bridge), while acetamidemethyl (Acm) was used for blocking the free thiol groups of the cysteine residues in the synthesis of the reduced peptide with the thiol groups permanently blocked.

Cleavage of the peptide–resin complexes was performed by treatment with trifluoroacetic acid/1,2-ethanedithiol/anisole/phenol/water (82.5:2.5:5:5:5 by volume) at room temperature for 2 h. After filtering to remove the resin, anhydrous diethyl ether (Sigma) at 4 °C was added to the soluble material to cause precipitation of the crude peptide, which was collected as a pellet by centrifugation at 1000 ×*g* for 15 min at room temperature. The crude peptide was solubilised in water and purified by RP-HPLC. The peptide with the disulphide bridge was obtained by air oxidation of cysteine residues as described elsewhere [10].

Synthetic Paulistine peptides (in oxidised form with a disulphide bridge and in reduced and acetoamidated forms), were purified by high performance liquid chromatography (HPLC, mod. LC 8A) using a Shim-Pack C-18 Prep-ODS (K) column (30 mm x 250 mm, 15 μm, Shimadzu) under isocratic elution with 45% (v/v) MeCN/H_2O [containing 0.05% (v/v) TFA] at a flow rate of 10 mL/min. The elution was monitored at 214 nm with a UV–vis detector (Shimadzu, mod. SPD-20A Prominence). The fractions were manually collected and dried using a lyophiliser (Heto). The homogeneity and correctness of the sequence of the synthetic peptides were assessed using a gas-phase sequencer PPSQ-21A (Shimadzu) based on automated Edman degradation chemistry and ESI-MS analysis.

2.6. Circular dichroism measurements

To evaluate conformational changes in the peptides induced by different membrane-mimetic environments, CD spectra were obtained at a peptide concentration of 20 μM in either bi-distilled water, 40% (v/v) 2,2,2-trifluoroethanol (TFE)/water, or sodium dodecyl sulphate solutions (SDS) above and below the critical micelle concentration (CMC) of SDS (8 mM and 165 μM SDS, respectively). CD spectra were recorded from 260 to 190 nm with a Jasco-710 spectropolarimeter (JASCO International Co. Ltd., Tokyo, Japan) calibrated routinely at 209 nm using a D-Pantolactone solution [11]. Spectra were acquired at 25 °C using a 0.5 cm path length cell at a scan speed of 20 nm/min, a bandwidth of 1.0 nm, a response of 0.5 s, and a resolution of 0.1 nm. Eight scans were acquired for each spectrum. Following a baseline correction, the observed ellipticity in θ (mdeg) was converted to mean residue ellipticity [Θ] (deg cm^2/dmol), using the relationship $[\Theta] = 100\ \theta/(l\ c\ n)$ where "l" is the path length in centimetres, "c" is the peptide millimolar concentration, and "n" is the number of peptidic bonds. Assuming a two-state model, the observed mean residue ellipticity at 222 nm (Θ^{obs}_{222}) was converted into an α-helix fraction (f_H) using the method proposed by Rohl and Baldwin (1998) [12] and previously described elsewhere [13].

2.7. Molecular modelling

The search for templates of the Paulistine sequence was performed with the Blastp tool [14] and the alignment was formatted and input into the programme. The structure of the homologous peptide, which was experimentally solved by NMR (PDB ID: 2KGH) [15], was selected from the Protein Data Bank (PDB) [16]. Synthetic peptide models were built with restraint-based modelling implemented in MODELLER [17]

using standard protocols for comparative protein structure modelling by the satisfaction of spatial restrains [18,19]. For each peptide, a total of 1000 models were created and the best ones were selected according to the MODELLER objective function [20] and stereochemical analysis with PROCHECK [21]. The sequence similarity between Paulistine and the template was 61% (identity 38%). The final models were selected with 100% of the residues in favoured regions of the Ramachandran plot, with the best values of the overall G-factor and lower values of energy minimisation. Both reduced and oxidised forms of Paulistine were modelled; the reduced peptide was modelled considering the acetamidemethylation of the thiol groups of cysteine. Pymol was used for the visualisation of the models of both forms of Paulistine [22].

2.8. Molecular dynamics simulations

The MD simulations were performed with the GROMACS 4.5.5 software package [23] using the GROMOS 96 force field 43a2 [24] and the flexible SPC (Simple Point Charge) water mode [25]. For TFE molecules in the simulation, the model and simulation conditions were applied as proposed by Fioroni et al. (2001) [26]. Simulations of both peptides were carried out in a cubic box containing TFE and water corresponding approximately to a mixture of 40:60% (v/v) TFE:water in which the minimum distance between the peptide surface and the box face was 1.0 nm length in all directions and neutralised with five Cl^- counterions. During the simulations, bond lengths within the peptides were constrained by the LINCS algorithm [27] and the SETTLE algorithm [28] was used to constrain the water geometry. In the initial MD simulation of both forms of Paulistine, all hydrogen atoms, ions, and water molecules were subjected to 500 steps of energy minimisation by steepest descent to remove close van der Waals contacts. Both systems were then submitted to a short molecular dynamics simulation with position restraints for a period of 2000 ps (ps). The final MD simulations were performed under the same conditions, except that the position restraints were removed after an interval of 20,000 ps. Energy minimisation and MD were carried out under periodic boundary conditions. The simulation was computed in the NPT ensemble at 300 K with Berendsen temperature coupling and a constant pressure of 1 atm with isotropic molecule-based scaling [29,30]. Temperature and pressure were modulated using coupling techniques [29] with coupling and isothermal compressibility constants of 0.01 ps (solvent and peptide) and 6.5×10^{-5} bar^{-1}, respectively. The electrostatic interactions between non-ligand atoms were evaluated by the particle mesh Ewald method [31]. Cutoff distances for the calculation of the Coulomb and van der Waals interactions were 1.0 and 1.4 nm, respectively. The convergences of the different simulations were analysed in terms of the radius of gyration (RG), root mean-square deviation (RMSD) from the initial structures of the models, and types of intermolecular hydrogen bonds. All analyses were performed on the ensemble of system configurations extracted at 0.5 ps time intervals from the simulation and the MD trajectory collection was initiated after 1 ns of dynamics to ensure a completely equilibrated evolution. The molecular visualisation was performed in the graphical environments VMD [32] and PyMOL [22].

2.9. Biological assays

2.9.1. Hemolytic activity

Washed rat red blood cells (WRRBC) were used to evaluate the hemolytic activity of the peptides. WRRBC were prepared by washing red blood cells of Wistar rats three times with physiological saline solution (NaCl 0.85% and $CaCl_2$ 10 mM). Aliquots of WRRBC were then incubated at 25 °C in the presence of each peptide for 120 min with gentle mixing. Samples were then centrifuged and the absorbances of the supernatants were measured at 540 nm. The absorbance measured from lysed WRRBC in the presence of 1% (v/v) Triton X-100 was considered to be 100%.

2.9.2. Mast cell degranulation activity

Mast cell degranulation activity was determined by measuring the release of β-D-glucosaminidase [33]. Mast cells were incubated in the presence of peptides for 15 min at 37 °C. After centrifugation, the supernatants were sampled for use in the β-D-glucosaminidase assay for a period of 6 h. After incubation, 50 μL of the supernatant solution was added to 150 μL of 0.2 M Tris and the absorbance was measured at 405 nm. The values were expressed as the percentage of total β-D-glucosaminidase activity from rat mast cell suspensions, relative to lysed mast cells in the presence of 0.1% (v/v) Triton X-100 (considered to be the 100% reference). The results were compared to the activities measured for the standard mast cell degranulating peptide HR-II (SIGMA).

2.9.3. Chemotaxis assays

Chemotaxis was assayed in a specific multi-chamber apparatus (NEUROPROBE) by using polymorphonucleated leukocytes (PMNL) obtained from subcutaneous inflammatory induction in Wistar rats as proposed by Falk (1980) [34]. The upper chambers were filled with 200 μL of a PMNL suspension (5×10^5 cells/mL in a 0.9% NaCl solution) and the lower chambers were filled with 400 μL of physiological saline solution containing various concentrations of the peptides (10^{-7} to 10^{-4} M). A polycarbonate membrane containing pores of 10 μm in diameter was placed between both chambers. The chemotaxis chamber was incubated at 37 °C for 1 h. After incubation and violet crystal staining, cells in the lower chamber were counted using a Neübauer chamber under a microscope. The results are expressed as the mean ± the S.D. of five experiments.

2.9.4. Antimicrobial activity

The minimal inhibitory concentrations (MIC) of the peptides were determined based on the methods described in [35]. The following microorganisms were used: *Staphylococcus aureus* (ATCC 6538), *Streptococcus pneumoniae* (ATCC 11733), *Bacillus cereus* (ATCC 11778), *Escherichia coli* (ATCC 1175) and *Pseudomonas aeruginosa* (ATCC 13388).

2.9.5. Hyperalgesic and edematogenic effects

Male Swiss mice, weighing between 25 and 30 g, were used throughout this study. Mice were housed under controlled humidity at a temperature of 22 °C ± 1 in a sound-attenuated room subject to a 12 h light–dark cycle. Food and water were available ad libitum and mice were taken to the testing room at least 1 h before the experiment. All behavioural testing was performed between 9:00 am and 4:00 pm. The mice were used only once. All experiments were in accordance with the guidelines for the ethical use of conscious animals in pain research, published by the International Association for the Study of Pain [36] and EC Directive 86/609/EEC for Animal Experiments. The procedures were approved by the Institutional Animal Care Committee at Butantan Institute (CEUAIB, protocol no. 567/09).

2.9.5.1. von Frey electronic pressure-meter paw tests for mice. Mice were placed in acrylic cages (12 × 10 × 17 cm high) with a wire grid floor 15–30 min before testing. During this adaptation period, the paws were poked 2–3 times. Before paw stimulation, the animals were quiet, without exploratory movements or defecation and not resting on their paws. In these experiments, we used a pressure-meter, which consisted of a hand-held force transducer fitted with a 0.5 mm^2 polypropylene tip (electronic von Frey anesthesiometer, IITC Inc., Life Science Instruments, Woodland Hills, CA, USA). The investigator was trained to apply the polypropylene tip perpendicularly to the central area of the hind paw with a gradual increase in pressure. A tilted mirror below the grid provided a clear view of the animal's hind paw. The test consisted of poking a hind paw to provoke a flexion reflex followed by a clear flinch response after paw withdrawal. In the electronic pressure-meter test, the intensity of the stimulus was automatically recorded when the paw was

withdrawn. The maximal force applied was 18 g. The stimulation of the paw was repeated until the animal presented two similar measurements. If the results were inconsistent (i.e., a great difference in the baseline response compared to the other animals of the experiment was observed), another animal was used. Hyperalgesic effect was induced by the injection by the intraplantar (i.pl.) route of either carrageenin (300 μg/50 μL) or peptides (10 and 30 μg/50 μL) into one of the hind paws. The results are reported as the Δ (delta) withdrawal threshold (g) which was calculated by subtracting the values obtained after the treatments from the first measurement (before treatment).

2.9.5.2. Evaluation of oedema. Oedema was induced by the injection of carrageenin (300 μg/50 μL) or peptides (10 and 30 μg/50 μL) into one of the hind paws by the intraplantar (i.pl.) route. The volume increase (oedema) of paws up to the tibio-tarsal articulation was measured using a digital paquimeter (Mitutoyo, CD-6 CSX-B model, Brazil). Indomethacin and Zileuton were administrated to evaluate the antiedematogenic effect. The difference between the values obtained for both paws expressed as percent increase in paw volume was used as a measure of oedema.

2.9.5.3. Evaluation of nociceptivity. For evaluation of the nociceptive activity of Paulistine and Acm-Paulistine, both peptides were dissolved in sterile saline (10 and 30 μg/50 μL) and administered by the i.pl. route into one of the hind paws of the mice. A hypodermic 26-G needle was inserted into the skin of the second footpad (to avoid back flow) and the tip of the needle was introduced until the central area of the hind paw was in the same place where either the filaments or the tip of the pressure meter were applied. The nociceptive activity was evaluated at different times (before treatment and 30, 60, 120 and 300 min after Paulistine and Acm-Paulistine application) and compared to the control. Carrageenin (Marine Colloids, 300 μg/50 μL) was diluted in sterile saline and used as positive control; sterile saline was used as a negative control. To assess the involvement of arachidonate metabolites in this phenomenon, different groups of rats were treated with either the cyclooxygenase inhibitor indomethacin (SIGMA, USA, 100 μg/25 μL in 0.1 M Tris–HCl buffer at pH 8.0) (control) or with the type 2 cyclooxygenase inhibitor Celecoxib (30 mg/kg administered by an oral route) 30 or 120 min (respectively) before the injection of the peptides [37]. The lipoxygenase inhibitor Zileuton (Abbott Laboratories, Zyflo®, USA) was diluted in an hydroalcoholic solution (10% ethanol) and assayed 60 min before injection of the peptides (100 mg/kg administered by an oral route) [38]. To evaluate the involvement of leukotriene receptors, Zafirlukast (SIGMA, USA) was diluted in 0.5% dimethyl sulfoxide (DMSO, SIGMA, USA) and administered by an oral route at 5.0 mg/kg. Animals injected with hydroalcoholic solution plus sterile saline was used as a control group.

2.10. Statistical analysis

Two-way analysis variance (ANOVA) was used to compare the groups and doses over all times. Three factors were analysed: treatments, time and time vs. treatment interaction. When a significant time vs. treatment interaction was detected, one-way ANOVA followed by the Tukey test was performed for each time point to distinguish dose effects. One-way ANOVA followed by the Tukey test was also used for dose–response curves for a single time point. The results with $p < 0.05$ were considered to be significant [39].

3. Results

3.1. Structural characterisation

A *P. paulista* venom extract (5 mg) containing approximately 3.5 mg of peptides was fractionated by reverse-phase HPLC resulting in the elution of thirteen fractions (designated 1 to 13 in Fig. 1A). Fractions 1 to 3 consisted of free amino acids and biogenic amines; fraction 4 was characterised as serotonin; fractions 5 to 9 were determined to be very low abundant venom components not previously characterised; and fractions 11 to 13 consisted of mastoparan peptides that have been biochemically and functionally characterised in previous publications [40,41]. The Paulistine peptide was identified in fraction 10 (Fig. 1A), which was then re-fractionated, resulting in the elution of four other peaks (designated as 10.1 to 10.4). Paulistine eluted at fraction 10.2 (Fig. 1B); the ESI/MS spectrum of this fraction is shown in Fig. 2A, where is possible to observe the peaks of m/z values 472.87, 590.83, and 787.44, corresponding to the molecular ions as $[M + 5H]^{+5}$, $[M + 4H]^{+4}$, and $[M + 3H]^{+3}$, respectively (Fig. 2A); the deconvolution of this spectrum revealed that the peptide present in this fraction presented a molecular mass of 2359.32 Da. Thus, the mass spectrometric analysis indicated that the peptide was pure enough to be sequenced through automated Edman degradation chemistry, which revealed the sequence SIKDKICKIIQAQCGKKLPFT-NH_2. This novel peptide from social wasp venom was named Paulistine.

The sequence of Paulistine determined by Edman degradation apparently possesses two cysteine residues at positions 7 and 14; thus, the connectivity between these residues was checked by ESI-IT-TOF-MS analysis. The peptide treated with dithiothreitol indicated a molecular mass of 2361.32 Da (results not shown), suggesting that both cysteine residues are connected to each other to form an intramolecular disulphide bridge (Fig. 3).

The ESI-IT-TOF-MS analysis of fraction 10.3 revealed the peaks of m/z 591.31, 788.08, and 1181.62, corresponding to the molecular ions as $[M + 4H]^{+4}$, $[M + 3H]^{+3}$, and $[M + 2H]^{+2}$, respectively (Fig. 2B); the deconvolution of this spectrum revealed that the peptide present

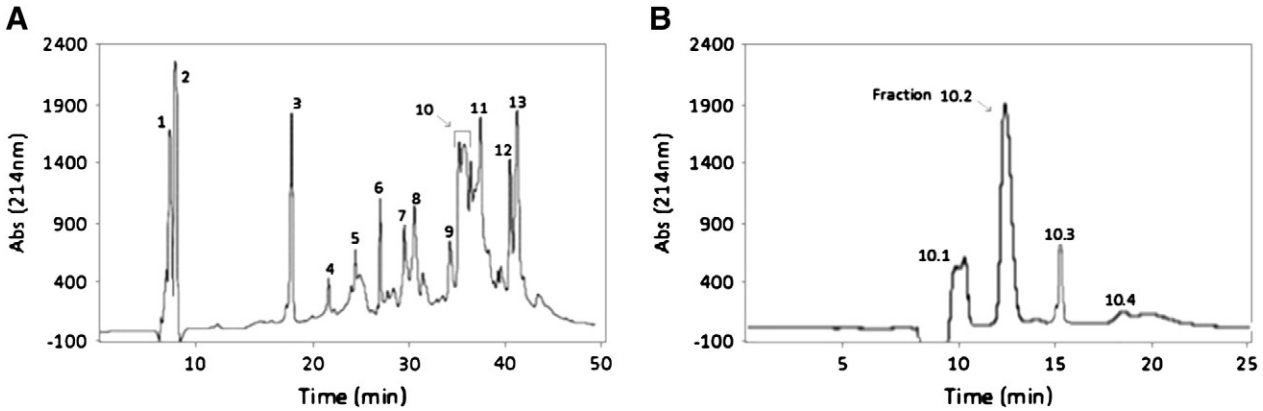

Fig. 1. A) Chromatographic fractionation of venom extract from *Polybia paulista* by RP-HPLC under a linear gradient from 5 to 60% (v/v) MeCN/H_2O (containing 0.1% TFA) at a flow rate of 2.0 mL/min over 60 min with UV monitoring at 214 nm. B) Re-chromatography of fraction 10 by RP-HPLC under an isocratic condition using 40% (v/v) MeCN/H_2O (containing 0.1%TFA) as the mobile phase with a flow rate of 2.0 mL/min over 20 min with UV monitoring at 214 nm.

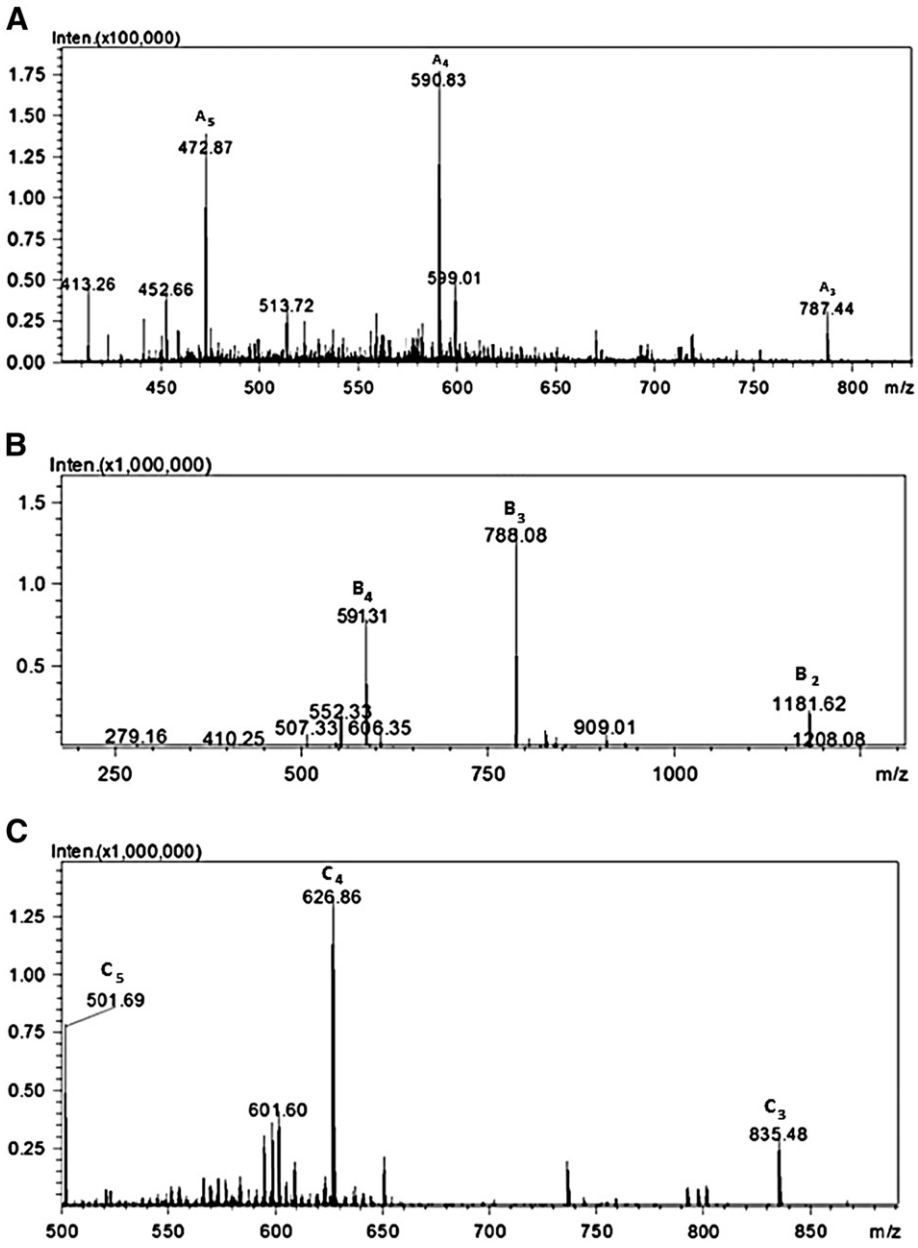

Fig. 2. MS^1 spectra, in the positive mode, of: (A) naturally oxidised Paulistine peptide present in fraction 10.2, showing the peaks of m/z 472.87, 590.83, and 787.44, corresponding to the molecular ions as $[M + 5H]^{+5}$, $[M + 4H]^{+4}$, and $[M + 3H]^{+3}$, respectively; (B) naturally reduced peptide present in fraction 10.3, showing the peaks of m/z 591.31, 788.08, and 1181.62, corresponding to the molecular ions as $[M + 4H]^{+4}$, $[M + 3H]^{+3}$, and $[M + 2H]^{+2}$, respectively; (C) reduced and acetamidemethylated peptide, where is possible to observe the peaks of m/z 501.61, 626.86, and 835.48, corresponding to the molecular ions as $[M + 5H]^{+5}$, $[M + 4H]^{+4}$, and $[M + 3H]^{+3}$, respectively.

in this fraction presented a molecular mass of 2361.32 Da. This peptide was also sequenced by Edman degradation chemistry and was found to correspond to the naturally occurring reduced form of Paulistine. The naturally oxidised peptide (fraction 10.2) is relatively stable, i.e., it is slowly converted to its reduced form, even under rest at 4 °C and protected from the light. However, the purified peptide from fraction 10.3 (naturally reduced) quickly oxidises spontaneously until achieve an equilibrium in a proportion of 1:4 (reduced: oxidised).

Because the amount of natural peptides recovered from the purification protocol was strongly biased by the detection of the reduced form (65 μg of the reduced peptide was recovered from fraction 10.3 compared to 280 μg of the oxidised peptide from fraction 10.2), Paulistine was chemically synthesised in its oxidised and reduced forms, as well as a reduced form in which the thiol groups from the cysteine residues were coupled to an acetamidemethyl moiety (Fig. 3). Peptides were manually synthesised in the solid-phase using an Fmoc strategy. Oxidised Paulistine was obtained by air oxidation after its cleavage from the resin. Synthetic peptides were individually purified by RP-HPLC (C18) using isocratic elution with 40% (v/v) MeCN containing 0.1% TFA. Oxidised Paulistine eluted at 9.75 min, while the reduced and acetamidemethylated forms (Acm-Paulistine) eluted at 9.20 min (Fig. 4). The accuracy of the sequences of the synthetic peptides was

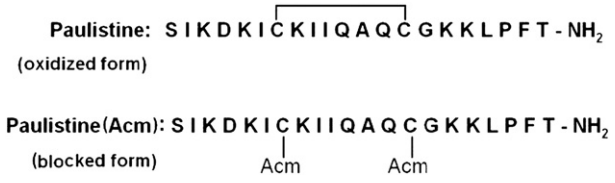

Fig. 3. Sequences of oxidised and reduced + acetamidemethylated Paulistine.

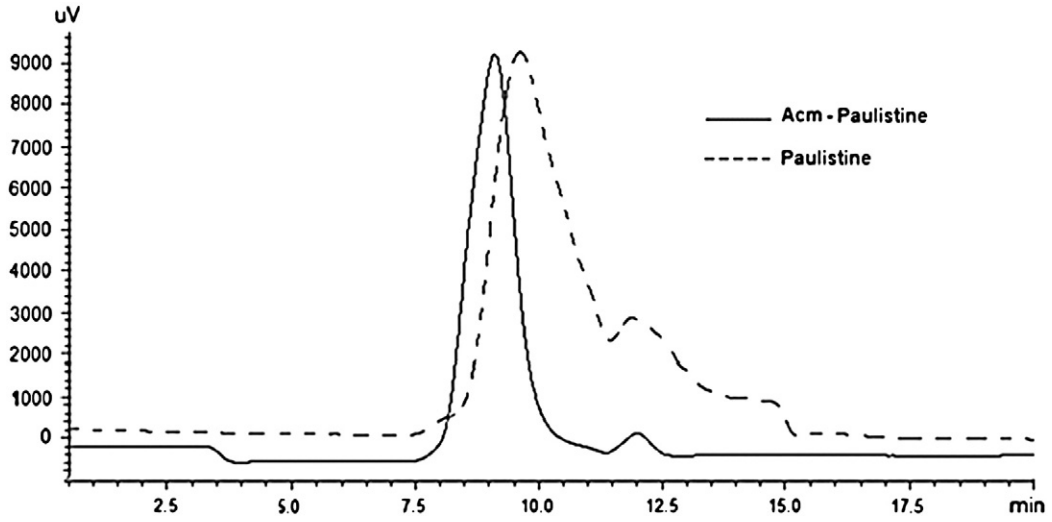

Fig. 4. Chromatographic profiles of the fractionation of synthetic oxidised ( ) and reduced + acetamidemethylated Paulistine under RP-HPLC (LC-8A) (- - - -) with a C-18 ODS-K Shim-Pack column (250 mm × 30 mm, 15 μm) under isocratic elution with 40% (v/v) MeCN (containing 0.1%TFA) as the mobile phase at a flow rate of 20.0 mL/min over 25 min with UV monitoring at 214 nm.

confirmed by automated Edman degradation chemistry and the homogeneity of the preparation was checked by ESI-IT-TOF-MS analysis; Fig. 2C shows the ESI/MS spectrum of the acetamidemethylated peptide, where it is possible to observe the peaks of m/z 501.61, 626.86, and 835.48, corresponding to the molecular ions as $[M + 5H]^{+5}$, $[M + 4H]^{+4}$, and $[M + 3H]^{+3}$, respectively. The deconvolution of this spectrum revealed a molecular mass of 2503.44 Da. The mass difference of 144 Da between the oxidised and the chemically modified form of the peptide corresponds to the introduction of the two acetamidemethyl groups into the peptide (2×72 Da $= 144$ Da). This strategy ensures that the reduced peptide will not oxidise the thiol groups to reform the disulphide bridges.

Considering the importance of secondary structure for understanding the biological activities of peptides, the secondary structures of Paulistine and Acm-Paulistine were investigated by CD spectroscopy. The CD spectra of the oxidised and reduced forms of Paulistine in water, 40% (v/v) TFE, and in the presence of SDS above and below the CMC of SDS (at 165 μM and 8 mM SDS, respectively) are shown in Fig. 5A. The corresponding spectra of Acm-Paulistine are shown in Fig. 5B.

Table 1 presents the molar ellipticity ([Θ222]) and the α-helix fractions (f_H^*) in the different environments. The α-helix fractions were calculated according to the two-state model [12], while the fractions of secondary structure were obtained by fitting the spectra with the CONTIN and SMP56 programmes within CDPro. It was found that the oxidised peptide possesses a lower helical content and higher strand content than the reduced and acetamidemethylated peptides.

The molecular models of Paulistine and Acm-Paulistine are shown in Fig. 6A and B, respectively. The analysis of the Ramachandran plot for these molecular models (supplementary information) revealed that 76.5% of the residues lie in the most favourable regions and 23.5% in the additionally allowed regions for the oxidised form of Paulistine. Meanwhile, the same analysis for the Acm-Paulistine model reveals that 76.5% of the residues lie in the most favourable regions, 17.6% in the additional allowed regions and 5.9% in generously allowed regions.

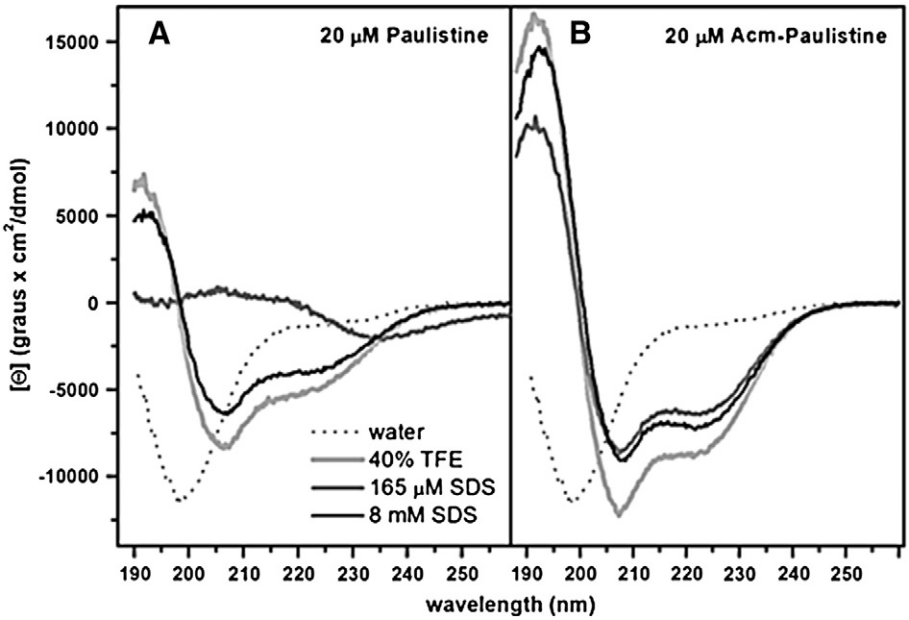

Fig. 5. CD spectra of (A) Paulistine and (B) Acm-Paulistine at 20 μM concentration acquired from 260 to 190 nm at 25 °C in the presence of water, 40% (v/v) TFE, 165 μM SDS and 8 mM SDS.

Table 1
Secondary structure evaluation of Paulistine and Acm-Paulistine in different environments: water, 40% (v/v) TFE solution, 165 μM SDS, and 8 mM SDS molar ellipticity ($[\Theta]_{222}$) and α-helix fractions (f_H^*) were calculated according to the two-state model [12], and the fraction content of helical (H), strand (S) and unordered (Unrd) structures was obtained from the fitting of spectra with the programme CDPro (CONTIN, SMP56).

	Paulistine					Acm-Paulistine				
	$[\Theta]_{222}$	f_H^*	H	S	Unrd	$[\Theta]_{222}$	f_H^*	H	S	Unrd
Water	−1324 ± 46	rc	–	–	–	−1328 ± 46	rc	–	–	–
40% TFE	−5088 ± 103	0,17	0.20	0.27	0.30	−8714 ± 121	0,30	0.35	0.15	0.29
165 μM SDS	−403 ± 187	–	0.05	0.45	0.28	−6412 ± 35	0,22	0.26	0.23	0.30
8 mM SDS	−4044 ± 66	0,13	0.19	0.28	0.30	−7206 ± 71	0,25	0.31	0.20	0.28

These results indicate that both models are adequate for structural studies. The molecular model of Paulistine possesses a small helix that is maintained and most likely stabilised by the disulphide bridge (Fig. 6A). The model of Paulistine is therefore more compact than the model of Acm-Paulistine, which possesses a more extended conformation (Fig. 6B) presumably due to the reduction of the thiol groups.

Despite the fact that these molecular models were considered adequate by the criteria considered above, they are static models. To obtain a more realistic idea about the structures of these peptides, the initial models were submitted to molecular dynamics analysis. The simulations were carried out both for oxidised and reduced forms of the peptide (Paulistine and Acm-Paulistine, respectively). The purpose of performing molecular dynamics was to investigate the stability of the secondary structure of the peptide with and without the cysteine bridge. This was performed by evaluating different variables:

i) The root-mean square deviation (RMSD) of the positions for all backbone C-α atoms as a function of simulation time (Fig. 7A). The analysis of the RMSD indicates that the reduced and acetoamidated forms of Paulistine show higher RMSD values when compared to oxidised Paulistine. The RMSD values for the C-α atoms of Acm-Paulistine rapidly increased initially during the MD simulation. However, this was followed by a period of relative stability for most of the remaining time of the MD simulation. The RMSD values for the C-α atoms of Paulistine remained stable throughout the MD simulation, suggesting that 20 ns of unrestrained simulation was sufficient to stabilise both peptides.
ii) The radius of gyration is the root mean square distance of the atoms in relation to the axes x, y and z of a specific molecule, and it can give an idea about the size and compactness of a molecule. In Fig. 7B it can be seen that the reduced peptide has a radius of gyration of 1.700 nm after 20 ns simulation, while the corresponding value for the oxidised form of the peptide was 0.800 nm after 4 ns simulation, which remained stable until 20 ns into the simulation. These results indicate that the presence of the disulphide bridge stabilises the peptide into a more compact molecular structure. The continuing increase in the radius of gyration during the simulation for the reduced peptide indicates that the absence of the disulphide bridge makes the structure of this peptide less stable and more expanded than that of the oxidised peptide.
iii) Analysis of the potential energy (Fig. 7C) shows that the peptides reached equilibrium and do not exhibit any asymptotic behaviour.
iv) The analysis of the prevalence of hydrogen bonds during the MD simulation shows that the number of hydrogen bonds in the oxidised peptide increased from 22 to 41 (with a rate value of 33), while in the reduced peptide the number of hydrogen bonds increased from 33 to 58 (with a rate value of 47). Despite this difference, the number of hydrogen bonds was relatively stable in both forms of the peptide during the simulation (Fig. 7D).

The surface charge representation of Acm-Paulistine (Fig. 8A) shows three regions of positive residues alternated with regions of negative residues in both faces of the molecule. It is easy to identify the acetamidemethylated thiol groups in this representation (Fig. 8A). The oxidised peptide (Paulistine) has a compact amphipathic structure with one face of the molecule presenting only positive residues, while the other face presents positive residues in two opposite borders with negative residues in the other borders and centre (Fig. 8B).

3.2. Biological characterization

The biological characterisation of Paulistine and Acm-Paulistine was evaluated by submitting these peptides to a series of activity assays to examine hemolysis, mast cell degranulation, chemotaxis of PMNLs, antibiosis, nociceptivity and edematogenic effect. Peptide stocks were maintained under lyophilized form; fresh solutions of each peptide form were prepared and immediately used to avoid to the conversion oxidised to reduced forms. Neither peptide caused hemolysis, mast cell degranulation or antibiosis (results not shown). However, chemotaxis

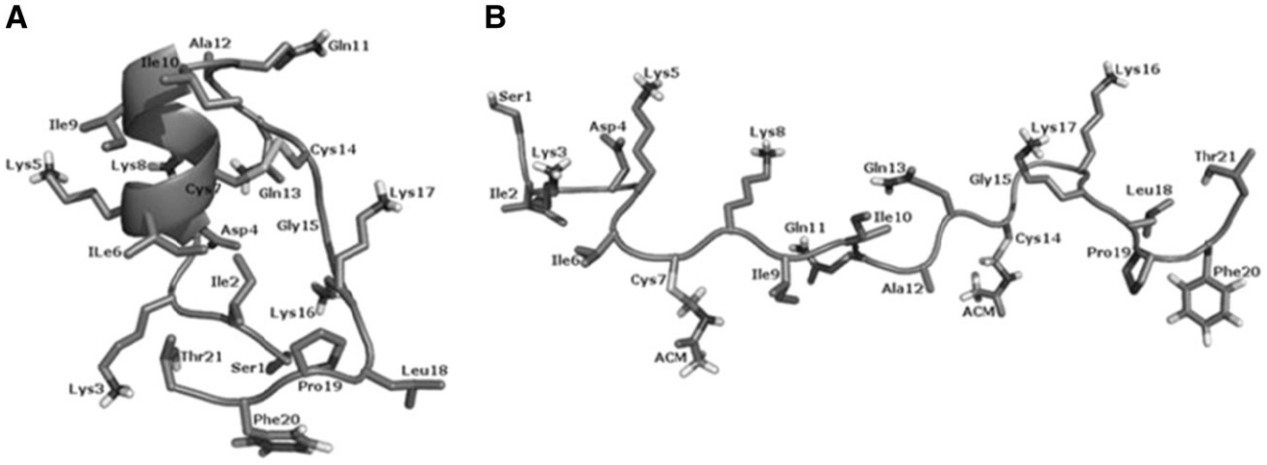

Fig. 6. Molecular models of A) Paulistine and B) Acm-Paulistine.

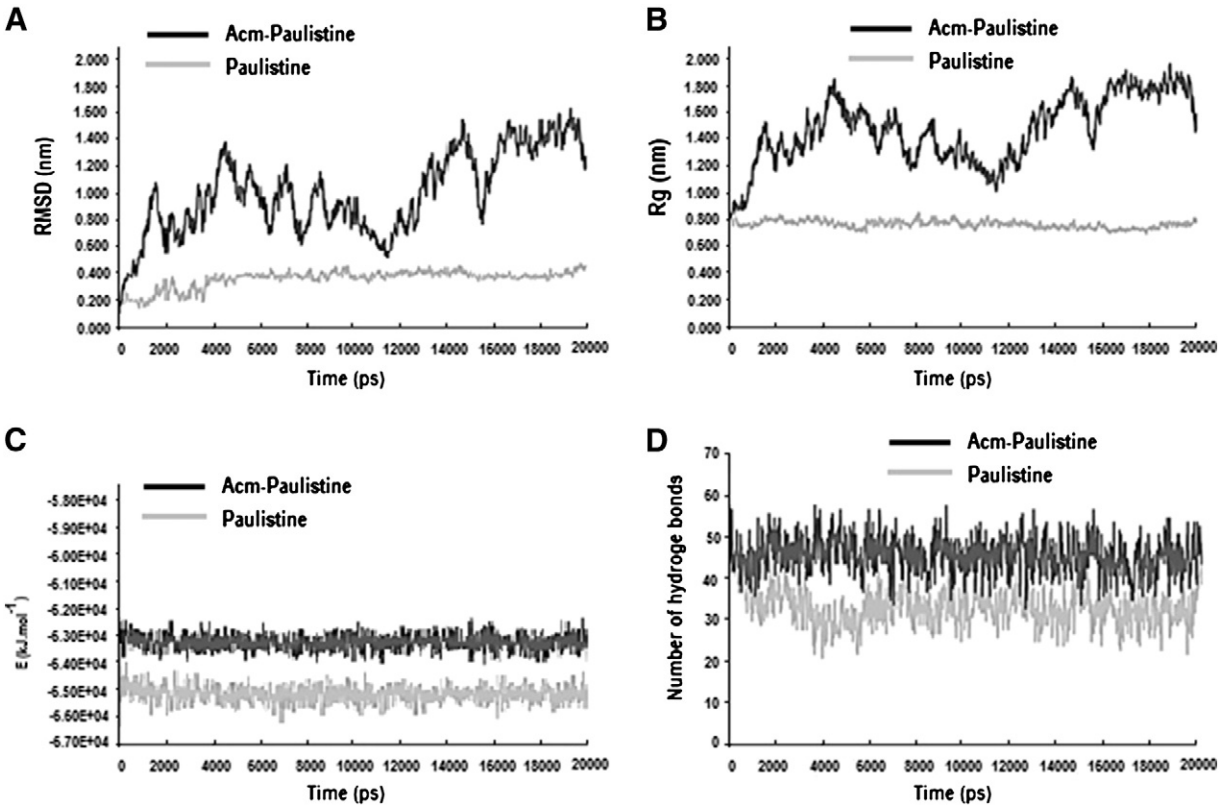

Fig. 7. Molecular dynamics simulations of Paulistine and Acm-Paulistine: A) root mean-square deviation (RMSD); B) radius of gyration (Rg); C) potential energy; and D) hydrogen bonds.

of PMNL cells was detected in response to both peptides. Different levels of chemotactic activity were observed with each peptide. Paulistine and Acm-Paulistine attracted 4.0×10^5 cells/mL and 1.8×10^5 cells/mL, respectively, at a concentration of 1×10^{-5} M (Fig. 9).

3.2.1. Hyperalgesic and edematogenic effects

The injection of 10 and 30 μg Paulistine (Fig. 10A) and Acm-Paulistine (Fig. 10C) caused a significant increase of nociception, characterised by hyperalgesia for both forms of Paulistine. The most intense effects for 30 μg Paulistine were observed between 30 and 120 min after peptide administration, while for Acm-Paulistine more intense effects were observed between 30 and 60 min. These phenomena disappeared within 300 min for Paulistine (Fig. 10A) and within 120 min for Acm-Paulistine (Fig. 10C). In both experiments carrageenin (Cg, i.pl., 300 μg) was used as a standard compound for positive nociception, while sterile saline was injected as control.

The injection of 10 and 30 μg of either Paulistine or Acm-Paulistine induced an increase in paw volume (Fig. 10B and D, respectively). The edematogenic effect of Paulistine was initiated after 30 min of its application in rats, while for Acm-Paulistine these effects were observed immediately after its application. It is important to note that the edematogenic effect caused by the injection of 30 μg Paulistine

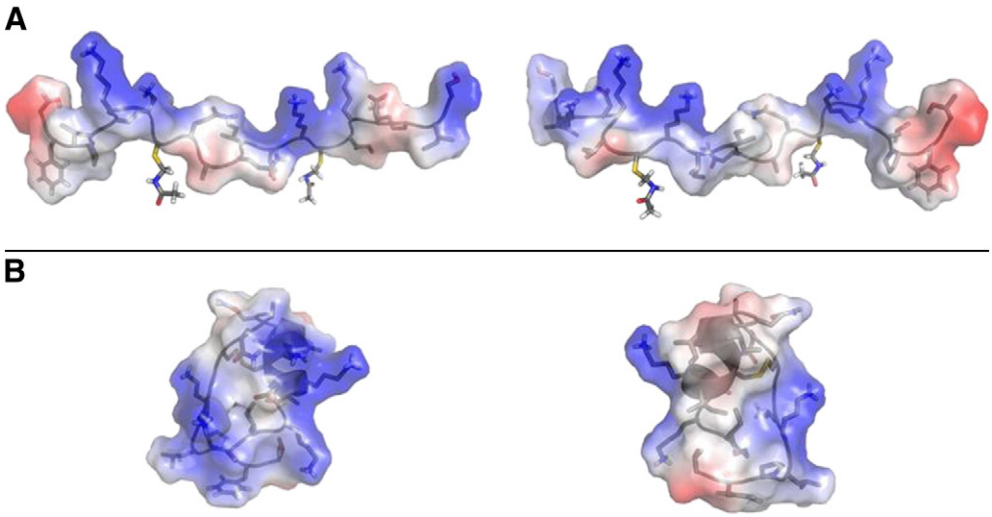

Fig. 8. Structural models of Acm-Paulistine (A) and Paulistine (B) as charge surface representations in two different molecular surfaces. Negative residues are shown in red and positive residues in blue.

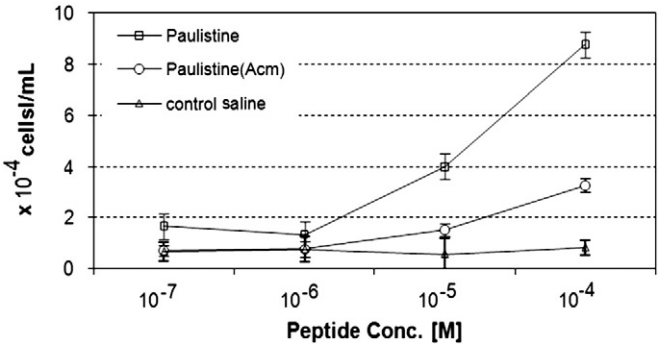

Fig. 9. Chemotaxis of PMNL cells for the peptides Paulistine and Acm-Paulistine at different concentrations. The values represent the mean ± S.D. (n = 5).

(Fig. 10 B) or Acm-Paulistine (Fig. 10D) was similar to that caused by carrageenin (the positive control); these phenomena disappeared in 300 min after the start of application for Paulistine and after 120 min for Acm-Paulistine.

3.2.2. Involvement of eicosanoids on hyperalgesic and edematogenic effects

Because both forms of the peptide induced hyperalgesia and edema effects, the next objective was to evaluate the involvement of prostanoids and lipid mediators derived from the cyclooxygenase and lipoxygenase pathways in the effects mentioned above. Mice were treated with either indomethacin (I, 100 mg i.pl.) — a cyclooxygenase pathway inhibitor or Zileuton (Z, 100 mg/kg taken by oral route in 500 μL) — a lipoxygenase pathway inhibitor, before the injection of Paulistine (30 μg i.pl.) and mechanical hyperalgesia was evaluated using an electronic von Frey instrument and edema formation was monitored using measurements with a digital paquimeter. The results shown in Fig. 11A revealed that Zileuton inhibited the hyperalgesia induced by Paulistine when compared with the control group (Paulistine/saline). On the other hand, indomethacin did not inhibit this phenomenon (I + Paulistine). Both Zileuton and indomethacin inhibited the edema induced by Paulistine compared to the control group (Fig. 11B). It is important to note that the effect of Zileuton was more prominent than indomethacin.

None of the drugs altered the pain threshold per se or edema in the animals treated (data not shown). The additional control groups consisted of animals treated with saline/Tris, saline/indomethacin, and saline/water/alcohol. These treatments did not interfere with the hyperalgesic and edematogenic effects in animals during the observation period (data not shown).

In a similar experiment described above, the results showed that indomethacin inhibited the hyperalgesia induced by Acm-Paulistine, while Zileuton did not inhibit this phenomenon (Fig. 12A). However, Zileuton and indomethacin both inhibited the edema induced by Acm-Paulistine (Fig. 12B). It is important to note that the effect of indomethacin was more prominent for Acm-Paulistine than for Paulistine.

3.2.3. Involvement of leukotriene receptors in the hyperalgesic and edematogenic effects of Paulistine

Because the results presented herein showed that Zileuton inhibited the hyperalgesia and edema induced by Paulistine, we decided to investigate the involvement of leukotriene receptors in these mechanisms. For this purpose, Zafirlukast (ZF), a leukotriene receptor antagonist [42], was injected (5 mg/kg in 300 μL of a DMSO 0.5% — vehicle taken by an oral route) prior to Paulistine injection (assigned as [ZF + Paulistine] in Fig. 13).

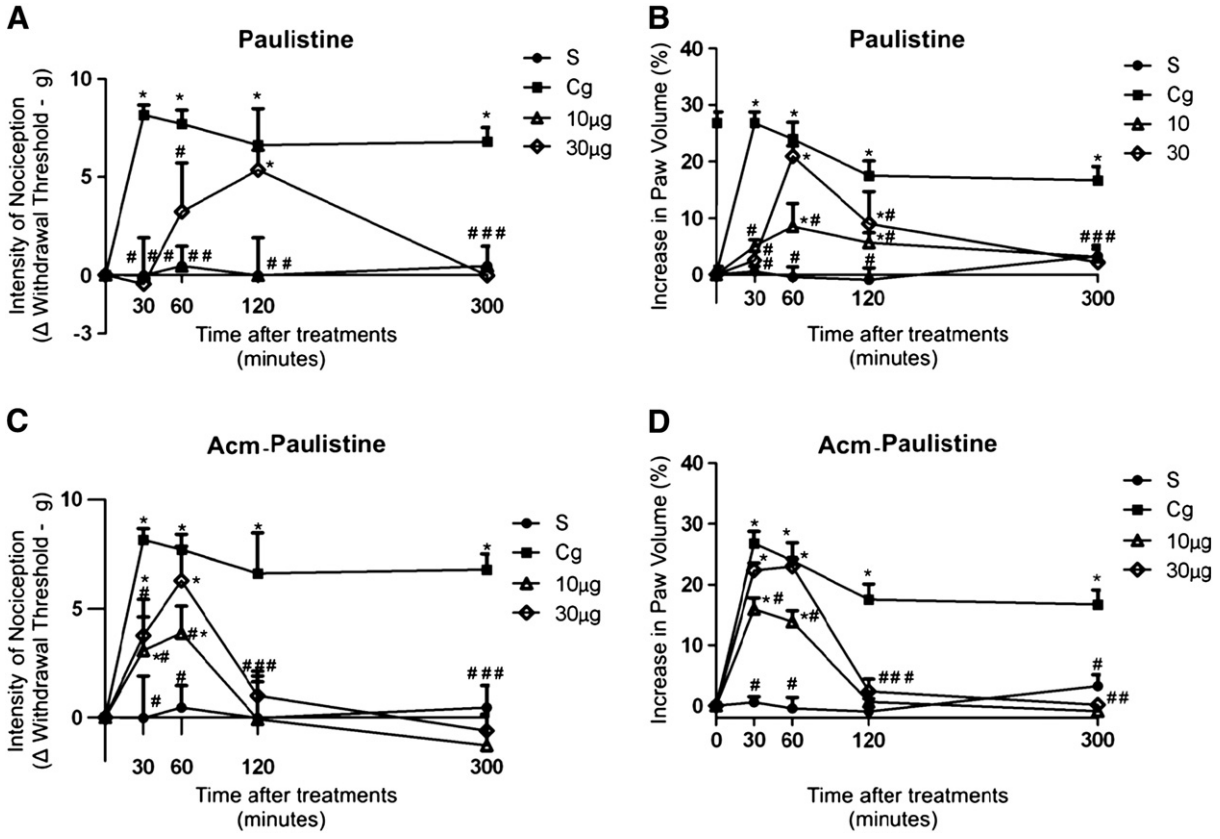

Fig. 10. Evaluation of the hyperalgesic and edematogenic effects of Paulistine and Acm-Paulistine. Paw threshold was estimated by the electronic von Frey device. The force needed to induce paw withdrawal was recorded as the pain threshold represented by delta (Δ) (A and C). Edematogenic effects were evaluated using a digital caliper paquimeter (B and D). The data were obtained at time 0 and at 30, 60, 120 and 300 min after Paulistine (A and B), Acm-Paulistine (C and D) (10 and 30 μg i.pl.), or carrageenin (Cg, 300 μg i.pl.) administration. The control group were animals injected with sterile saline (S). The results are expressed as the mean ± SEM of 5 animals per group. *$p < 0.001$ significant difference from the mean values of the saline (S) group; #$p < 0.001$ significant difference from the mean values of the carrageenin (Cg) group.

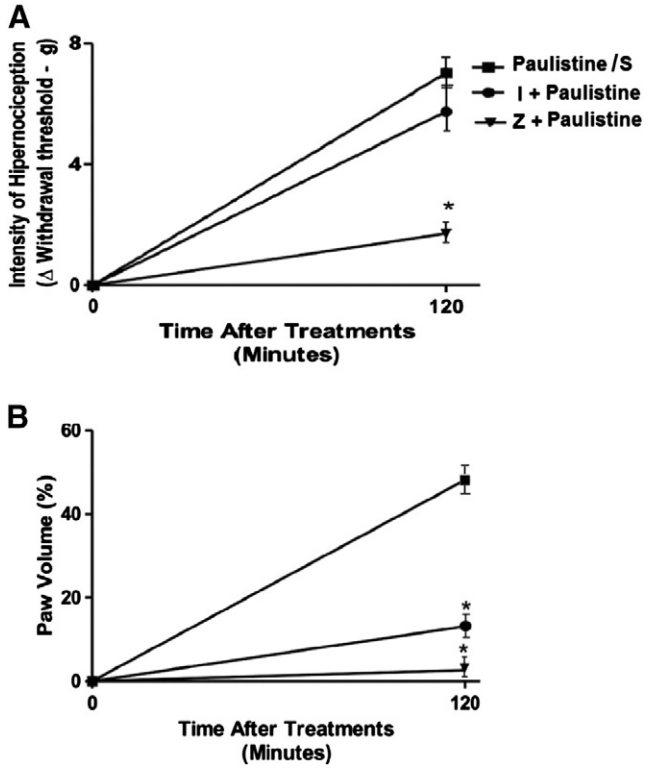

Fig. 11. Involvement of eicosanoids on the hyperalgesic and edematogenic effects of Paulistine. The paw threshold was estimated in the electronic von Frey device. The force needed to induce paw withdrawal was recorded as the pain threshold represented by delta (Δ) (A). Edematogenic effects were evaluated using a digital paquimeter (B). The data were obtained at time 0 and 60 min after Paulistine (30 μg i.pl.) administration. Indomethacin (I, 100 μg i.pl.) and Zileuton (Z, 100 mg/kg, by oral route in 500 μL) were administered at 30 min and 1 h before peptide injection, respectively. The control group were animals injected with [Paulistine/saline]. The results are expressed as the mean ± SEM of five animals per group. *$p < 0.001$ significant difference from the mean values of [Paulistine/saline].

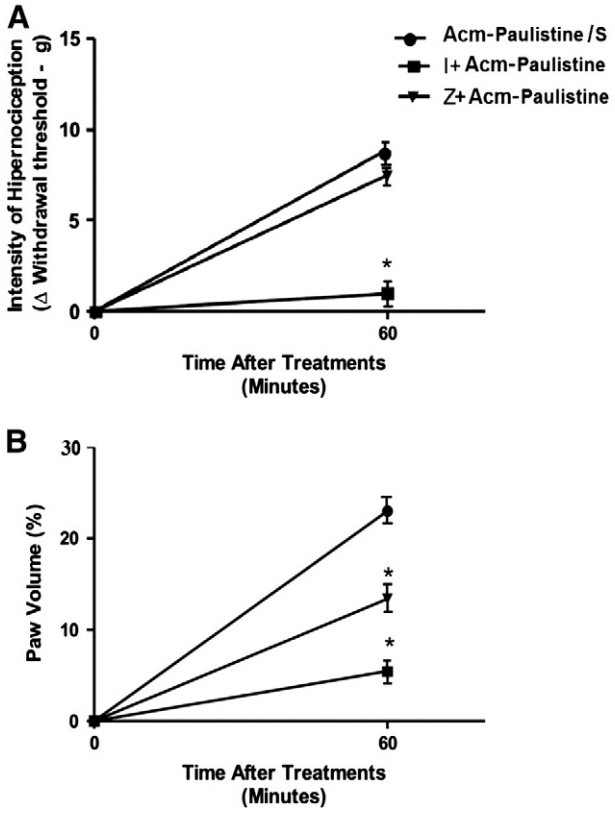

Fig. 12. Involvement of eicosanoids in the hyperalgesic and edematogenic effects of Acm-Paulistine. The paw threshold was estimated in the electronic von Frey device. The force needed to induce paw withdrawal was recorded as the pain threshold represented by delta (Δ) (A). Edematogenic effects were evaluated using a digital paquimeter (B). The data were obtained at time 0 and 60 min after Acm-Paulistine (30 μg, i.pl.) administration. Indomethacin (I, 100 μg, i.pl.) [I + Acm-Paulistine] and Zileuton (Z, 100 mg/kg, by oral route in 500 μL) [Z + Acm-Paulistine] were administered at 30 min and 1 h, respectively, before peptide. The control group were animals injected with saline + Acm-Paulistine. The results are expressed as the mean ± SEM of five animals per group. *$p < 0.001$ significant difference from the mean values of [Acm-Paulistine/saline].

The results shown in Fig. 13A indicate that Zafirlukast inhibited the hypernociceptive effect of Paulistine when compared to the group that received Paulistine/saline; the group treated with a 0.5% (v/v) Paulistine/DMSO showed no difference from the group that received Paulistine/saline. Zafirlukast did induce a significant blocking of edema induced by Paulistine (Fig. 13B). The group treated with a 0.5% DMSO vehicle [Paulistine/DMSO] showed no difference from the control group ([Paulistine/saline]).

3.2.4. Effect of Celecoxib on hyperalgesia and edema induced by Acm-Paulistine

Taking into account that Acm-Paulistine induced a hyperalgesic effect in which prostaglandins are important mediators and the fact that the cyclooxygenase inhibitor indomethacin inhibited this phenomenon, the next objective was to assess whether the generation of prostanoids is dependent on the activity of the enzyme cyclooxygenase type II. For this purpose, mice were previously treated with Celecoxib (C, 30 mg/kg, administered by oral route), a selective inhibitor of the enzyme cyclooxygenase type II, before injection of the Acm-Paulistine (P, 30 μg, i.pl.) and then evaluated on the mechanical hyperalgesia test [C + Acm-Paulistine]. The results shown in Fig. 14A reveal that Celecoxib inhibited the hyperalgesia induced by Acm-Paulistine when compared to the control group which received Acm-Paulistine/saline. Another objective of this investigation was to evaluate the involvement of cyclooxygenase type II on the edematogenic effect of Acm-Paulistine. The results shown in Fig. 14B indicate that Celecoxib caused a decrease in paw volume of animals when compared to the control group.

4. Discussion

Amongst the venoms of social Hymenoptera insects, the polycationic peptides generally represent the most abundant types of peptide toxins, which are represented by mast cell degranulators, hemolysins, antibiotic components and chemotactic agents. While in honeybee venoms the occurrence of peptides with disulphide bridges, such as Apamine, Tertiapine, and MCD-Peptide, is relatively common [43], in social wasp venoms there is a single report of a peptide containing a disulphide bridge, the toxin Sylverin, which was poorly characterised structurally and functionally [9].

A previous study also reported the presence of Paulistine occurring naturally both in oxidised and reduced forms in the venom of the neotropical social wasp *P. paulista* [3]. Thus, this study presents the structural characterization of Paulistine in its synthetic form, both with the disulphide bridge (oxidised) and in its reduced form (i.e., without the disulphide bridge, which was blocked by acetamidemethylation of the thiol groups) to prevent the re-oxidation and formation of the Cys–Cys disulphide bridge. The present manuscript focuses on the importance of the disulphide bridge for the molecular structure and biological activity of Paulistine.

The secondary structures of Paulistine and Acm-Paulistine were investigated by CD spectroscopy; spectra of both of these peptides in water (Fig. 5A and B, respectively) are characteristic of unordered conformations. In a medium composed of 40% (v/v) TFE and also in 8 mM SDS, the presence of two negative dichroic bands was observed, which is consistent with the induction of α-helix conformations in these

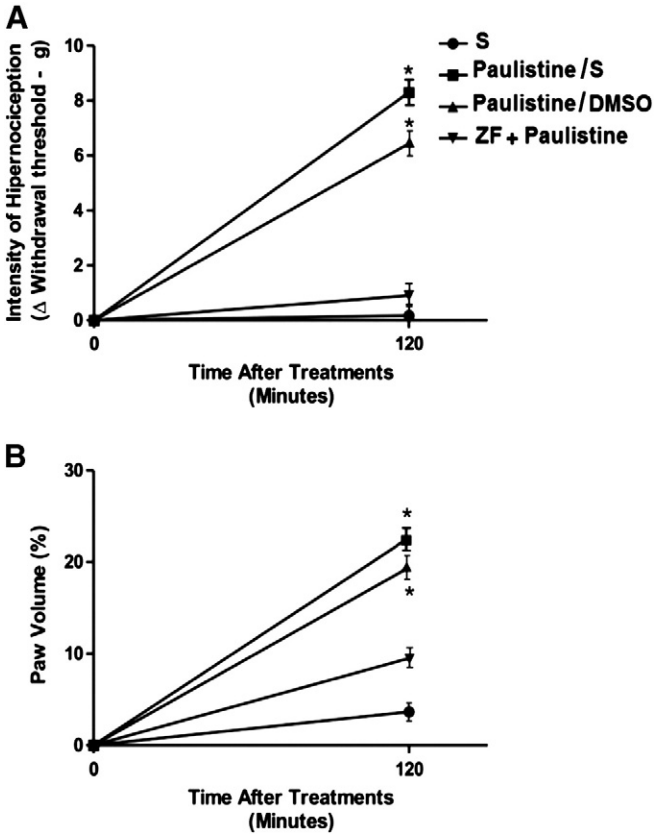

Fig. 13. Involvement of leukotriene receptors in hyperalgesia and edema induced by Paulistine. The paw threshold was estimated in the electronic von Frey device. The force needed to induce paw withdrawal was recorded as the pain threshold represented by delta (Δ) (A). The edematogenic effect was evaluated using a digital paquimeter (B). Data were obtained at time 0 and 60 min after Paulistine (P, 30 μg, i.pl.) administration. Zafirlukast (ZF, 5 mg/kg, by oral route), an antagonist of the leukotriene receptor, was administered before Paulistine administration [ZF + Paulistine]. The reference groups were animals injected with [Paulistine/saline] and [Paulistine/DMSO]. The results were expressed as the mean ± SEM of five animals per group. *$p < 0.001$ significant difference from the mean values of [Paulistine/saline] and [Paulistine/DMSO].

peptides. Nevertheless, the negative bands observed for Paulistine show a slight deviation (207 and 223 nm) from the characteristic values usually obtained for an α-helix of 208 and 222 nm, which were observed for Acm-Paulistine. SDS below the CMC tends to induce β-sheet conformations and mimics the core environment of proteins [44]. Sequences with either lower helical propensities or which show a tendency to form aggregates will deviate from the helical pattern. The CD spectra obtained in this environment clearly differentiate these peptides: Acm-Paulistine shows the characteristic helical profile, while Paulistine presents lower helical content than its analog in anisotropic and membrane-mimetic environments.

Table 1 presents the molar ellipticity ([Θ222]) and the α-helix fraction (f_H*) calculated according to the two-state model [12], in addition to the data obtained by the fitting of the spectra with CDPro (CONTIN, SMP56) programmes in the different environments. The data obtained with the help of CDPro programmes shows slightly higher helical contents (regular and distorted α-helical content) than the analysis made according to the two-state model for both peptides. This analysis also shows that Paulistine possesses a higher content of strand structures than Acm-Paulistine. Both peptides possess roughly the same amount of unordered and turn structures (22%; data not shown in Table 1).

The analysis of the Ramachandran plot for each peptide (shown in the Supplementary Results) reveals that both molecular models are structurally reliable (Fig. 6A and B). Considering that the molecular models created are generally static ones, a molecular dynamics (MD) analysis of the models generated for Paulistine and Acm-Paulistine was performed to investigate the stability of the peptide with and without a disulphide bridge. To monitor the progress of conformational changes of the peptides and to check the stability of its secondary structure elements during the simulation, the root-mean square deviation (RMSD) of the positions for all the α-carbons of each peptide backbone was evaluated as a function of simulation time. Analysis of the RMSD indicates that Acm-Paulistine possesses RMSD values higher than those observed for Paulistine over the entire 20 ns of simulation (Fig. 7A). Accordingly, the Paulistine structure appears to be more compact and stable than the structure of Acm-Paulistine as shown in Fig. 7B, which suggests that the disulphide bridge gives stability to the peptide. Analysis of the potential energy of both molecules (Fig. 7C) shows that both peptides reached equilibrium and did not exhibit any asymptotic behaviour. The analysis of the prevalence of hydrogen bonds during the MD simulation shows that the rate number of hydrogen bonds for Paulistine is smaller than the rate number determined for Acm-Paulistine; despite this difference the number of hydrogen bonds is relatively constant for both peptides all over the simulation, indicating the stability of the models (Fig. 7D).

When the molecular models of both forms of Paulistine were represented in the charge surface mode it becomes clear that the molecules of both peptides present two well distinguishable surfaces (Fig. 8A and B).

Biological assays showed that neither peptides induced hemolysis, mast cell degranulation, or even antimicrobial activity, but both peptides

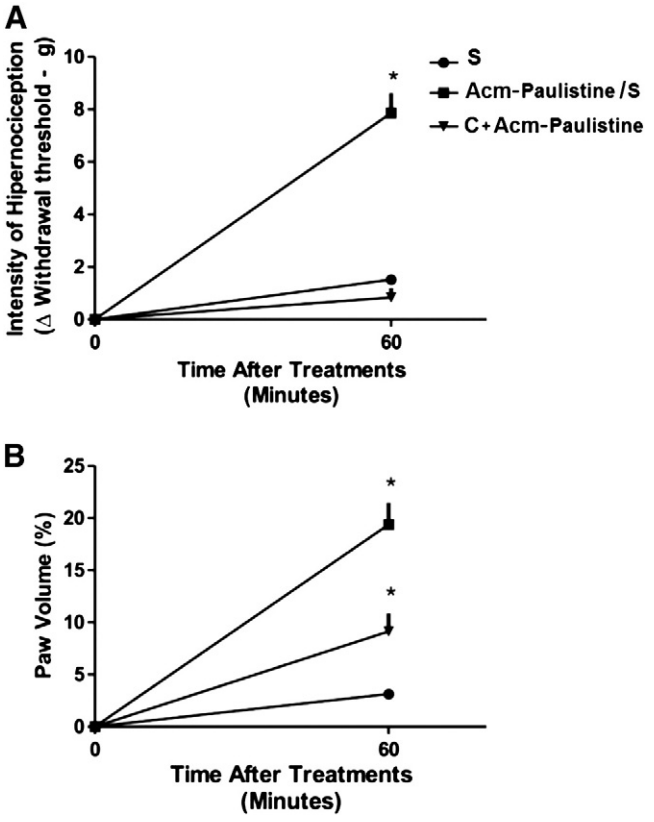

Fig. 14. Effect of Celecoxib on hyperalgesia and edema induced by Acm-Paulistine. The paw threshold was estimated in the electronic von Frey device. The force needed to induce paw withdrawal was recorded as the pain threshold represented by delta (Δ) (A). The edematogenic effect was evaluated using a digital paquimeter (B). The data were obtained at time 0 and 60 min after Acm-Paulistine (P-Acm, 30 μg, i.pl.) administration. Celecoxib (C, 30 mg/kg, by oral route), a selective inhibitor of enzyme cyclooxygenase type II, was administered 120 min before Acm-Paulistine administration [C + Acm-Paulistine]. The reference group were animals injected with Acm-Paulistine/saline, and the control group were animals injected with saline alone [S]. The results were expressed as the mean ± SEM of five animals per group. *$p < 0.001$ significant difference from the mean values of [Acm-Paulistine/saline], and [S].

induced high chemotaxis in PMNLs, which suggests the involvement of the oxidised and reduced forms of Paulistine in the inflammatory processes.

Pain induced by Hymenoptera venoms may be intense, lasting for several hours and burning for a few days [45]. Considering the algogenic and inflammatory role played by wasp venom toxins, Paulistine and Acm-Paulistine were submitted to assays of hyperalgesia and edematogenesis. The assay of hyperalgesia demonstrated that Paulistine and Acm-Paulistine induced pain at the same intensity, but at different times after their administration to the model animals. The hyperalgesia caused by Acm-Paulistine achieved its maximum activity 60 min after injection, while for Paulistine this maximum was observed 120 min after peptide administration (Fig. 10A to D). Thus, the hyperalgesia caused by Acm-Paulistine is faster than the action of the oxidised peptide. A similar effect was also reported for the edematogenic actions of Paulistine and Acm-Paulistine, i.e., both forms of the peptide presented the same intensity of edema formation; however, the action of Acm-Paulistine is faster, but short-lasting than that caused by Paulistine.

It is important to note that Zileuton (a lipooxygenase inhibitor) inhibited the hyperalgesia induced by Paulistine, but indomethacin did not, suggesting that some type of lipid mediator is involved in the phenomenon of hyperalgesia induced by Paulistine (Fig. 11A and B). The opposite occurred for Acm-Paulistine (Fig. 12A and B). Thus, the next objective was to assess whether this effect was mediated by a leukotriene receptor. The use of the compound Zafirlukast inhibited the hyperalgesia caused by Paulistine, demonstrating the involvement of leukotriene receptors in this activity (Fig. 13A and B).

In parallel, the investigation of the hypernociceptive effect of Acm-Paulistine demonstrated that this effect most likely occurs through interaction with the cyclooxygenase type II pathway, with the possible participation of prostanoids because Celecoxib counteracted the hyperalgesia caused by the reduced/acetamidemethylated peptide (Fig. 14A and B).

These data taken together suggest that distinct mechanisms mediate the nociceptive effects observed for Paulistine and Acm-Paulistine; apparently, both prostanoids and the lipid mediators seem to be involved with the nociceptive effects observed for these peptides. Prostaglandins (PGs) intensify the effect of pain indirectly through the actions of other agents, such as 5-hydroxytryptamine or bradykinin. The PGs of -E and -F series are released in inflammation, as well during tissue ischemia [46].

The lipoxygenase route results in the leukotriene formation, including leukotriene B4 (LTB4), eicosatetranoic acid 5-oxo-6E, 8Z, 11Z, 14Z and cysteinyl leukotrienes (LTC4, LTD4, LTF4 and LTE4), as well in the activation of four leukotriene receptors (BLT1, BLT2, cysLT1 and cysLT2). Leukotrienes are produced by many inflammatory cells, particularly mast cells, basophils, eosinophils, neutrophils and macrophages [46]. Zileuton, is the only drug commercially available as inhibitor of 5-lipoxygenase pathway; it blocks the production of LTB4 [46]. The biological actions of cysteinyl leukotrienes are mediated by the stimulation of CysLT1-receptors, which is competitively inhibited by Zafirlukast. Thus, while Zileuton inhibits the leukotriene synthesis, Zafirlukast blocks the leukotriene receptors [47].

Moreover, both Zileuton and indomethacin inhibited the edema caused by Paulistine and Acm-Paulistine, respectively, suggesting that both prostanoids and lipid mediators mediate this phenomenon. The results of the present study show that, with regard to the edematogenic effect, the most prominent inhibition was caused by Zileuton with Paulistine and indomethacin with Acm-Paulistine.

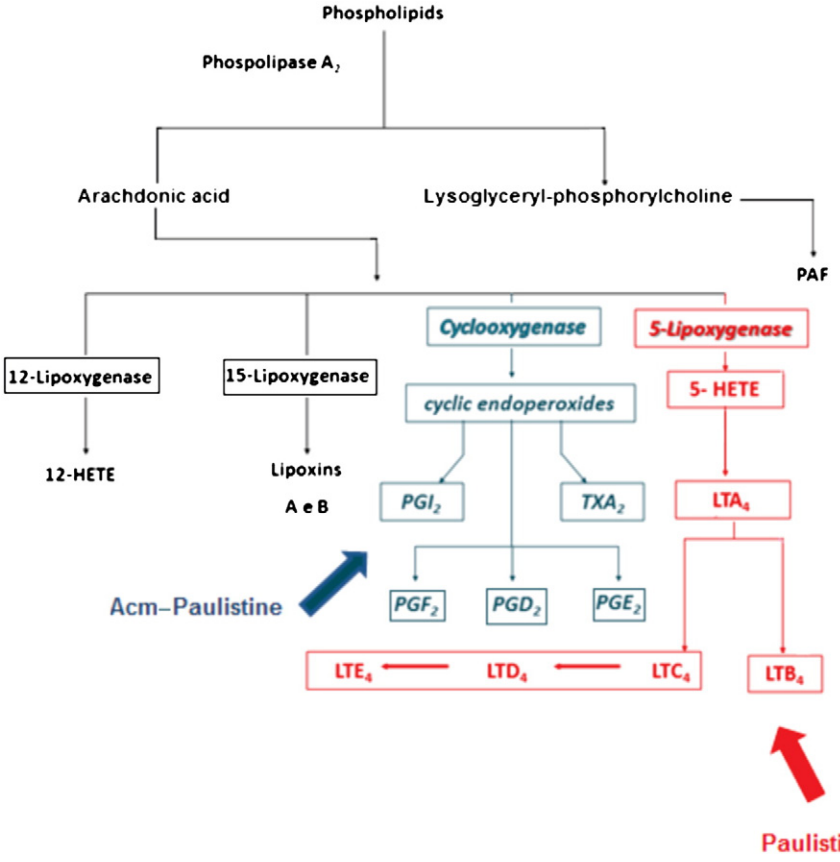

Fig. 15. A simplified scheme summarising the mechanisms involved in the nociceptive effect of Paulistine and Acm-Paulistine on the generation of prostanoids and other eicosanoids by arachidonic acid metabolism. Blue pathway and arrow — the cyclooxygenase pathway mediates the nociceptive mechanisms involved in mediating the effect of Acm-Paulistine; red pathway and arrow — the lipoxygenase pathway mediates the nociceptive mechanisms involved in mediating the effect of Paulistine. HETEs: hydroxyeicosatetraenoic acids; 12-HETE: 12-hydroxyeicosatetraenoic acid; 5-HETE: 5-hydroxyeicosatetraenoic acid; TXA_2: thromboxanes; PGF_2, PGD_2, PGE_2 and PGI_2: prostanoids; PAF: platelet-activating factor; LTE_4, LTD_4, LTC_4, LTB_4 and LTA_4: leukotrienes.

It is important to point out that our results demonstrated that there is no direct relationship between the development of hyperalgesia and edema caused by Paulistine and Acm-Paulistine. The mechanisms involved in these effects are different from each other, showing the involvement of prostanoids in the hyperalgesic process or the involvement of lipid mediators in the edematogenic effects (or vice-versa).

The inflammatory process is often associated with hyperalgesia and pain. Hyperalgesia can be defined as a pathophysiological manifestation resulting from sensitization of nociceptors and is a key event in the development of inflammatory pain. The hypersensitive inflammatory pain is the result of alterations in signal transduction in peripheral terminals (nociceptors) of high activation threshold and in excitability in the central nervous system [48].

Moreover, it was also reported divergence between the development of hyperalgesia and edema, induced by the venom of *Phoneutria nigriventer* [49]; this venom contains histamine and serotonin which could interfere with sensorial neuroactivities, and therefore could contribute with for its algogenic effect [50]. It was also reported that different mechanisms are involved in the development of hyperalgesia and edema induced by the venom of *Bothrops asper*, in which hyperalgesia was quickly controlled by drugs endowed with anti-inflammatory activity [51].

It is important to consider that chemical blockage caused by the acetamidemethylation of the thiol groups of cysteine residues caused small structural changes, which in turn may have affected some physicochemical properties of the Paulistine. Thus, the presence of two free thiol groups in the peptide would allow dipole–dipole interaction with the specific receptor of the reduced form of Paulistine. The insertion of Acm-group at this position to block the oxidation of thiol groups certainly affected the native structure and its possible interaction with the specific receptor, and consequently the profile of the biological activities of Acm-Paulistine. Thus, the dissociation of the hyperalgesy from the edematogenic effect when the actions of Paulistine and Acm-Paulistine are compared to each other, may be resulting from the influence of the introduction of Acm-group in the profile of structure–activity of Paulistine.

5. Conclusion

The results of the present investigation revealed an interesting example of two different conformations of the same peptide (Paulistine) coexisting at equilibrium in wasp venom, based on the maintenance of a balance between the oxidised and reduced forms of the thiol groups from the two cysteine residues in the peptide sequence.

Thus, the results of the present investigation suggest that the venom of *P. paulista* has a naturally oxidised form of the peptide Paulistine, which possesses a more compact structure due to the presence of a disulphide bridge, in a conformation that causes hyperalgesia, apparently favouring its interaction with receptors involved in lipid mediators metabolism at level of 5-lipoxygenase pathway (Fig. 15). The present results do not permit to know if the naturally reduced form of Paulistine has a different, or a similar biological activity as the Acm-Paulistine; however, the in-vitro reduced and acetamidemethylated form, which exists in a more expanded conformation, also causes hyperalgesia, but this chemically modified form of Paulistine seems to act at level of receptors involved with the prostanoid metabolism at level of cyclooxygenase type II pathway (Fig. 15). This way, Paulistine and Acm-Paulistine may be used as interesting tools to investigate the mechanisms of pain and inflammation in future studies.

Conflict of interest

The authors declare no conflicts of interests.

Acknowledgements

This research is supported by grants from FAPESP (BIOprospecTA Proc. 2011/51684-1), CNPq and Instituto Nacional de Ciência e Tecnologia de Investigação em Imunologia-iii (INCT/CNPq-MCT) and CAPES (Rede Nanobiotec-Brasi). MSP and JRN are researchers for the Brazilian Council for Scientific and Technological Development (CNPq).

Appendix A. Supplementary data

Supplementary data to this article can be found online at http://dx.doi.org/10.1016/j.bbagen.2013.08.024.

References

[1] B.M. De Souza, M.S. Palma, Monitoring the positioning of short polycationic peptides in model lipid bilayers by combining hydrogen/deuterium exchange and electrospray ionization mass spectrometry, Biochim. Biophys. Acta Biomembr. 1778 (2008) 2797–2805.
[2] S. Turillazzi, G. Mastrobuoni, F.R. Dani, G. Moneti, G. Pieraccini, G. La Marca, G. Bartolucci, B. Perito, D. Lambardi, V. Cavallini, L. Dapporto, J. Am. Soc. Mass Spectrom. 17 (2006) 376–383.
[3] M.S. Palma, Insect venom peptides, in: A. Kastin (Ed.), Handbook of Biologically Active Peptides, Academic Press, San Diego, 2006, pp. 409–417, (Chapter 56).
[4] L.D. Santos, J.R.A.S. Pinto, A.R.S. Menegasso, D.M. Saidemberg, A.M.C. Garcia, M.S. Palma, Proteomic profiling of the molecular targets of interactions of the mastoparan Polybia MP-III at the level of endosomal membranes from rat mast cells, Proteomics 12 (2012) 2682–2693.
[5] M.S. Palma, M.R. Brochetto-Braga, Biochemical variability between venoms from different honey bees (*Apis mellifera*) races, Comp. Biochem. Physiol. 106 (1993) 423–427.
[6] N.B. Baptista-Saidemberg, D.M. Saidemberg, M.S. Palma, Chemometric analysis of Hymenoptera toxins and defensins: model for predicting the biological activity of novel peptides from venoms and hemolymph, Peptides 32 (2011) 1924–1933.
[7] N.B. Baptista-Saidemberg, D.M. Saidemberg, M.S. Palma, Profiling the peptidome of the venom from the social wasp *Agelaia pallipes pallipes*, J. Proteomics 74 (2011) 2123–2137.
[8] B.E.C. Banks, R.A. Shipolini, Chemistry and pharmacology of honeybee venoms, in: T. Piek (Ed.), Venoms of Hymenoptera: Biochemical, Pharmacological and Behavioral Aspects, Academic Press, London, UK, 1986, pp. 329–416.
[9] K. Dohtsu, K. Hagiwara, M.S. Palma MS, T. Nakajima, Isolation and sequence analysis of peptides from the venom of *Protonectarina sylveirae* (Hymenoptera, Vespidae) (I), Nat. Toxins 1 (1993) 271–276.
[10] F. Albericio, I. Annis, M. Royo, G. Barany, Preparation and handling of peptides containing methionine and cysteine, in: C. Cheng, P.D. White (Eds.), Fmoc Solid Phase Peptide Synthesis: A Practical Approach, Oxford Univ. Press, Oxford, U.K., 2004, pp. 77–114.
[11] T. Konno, H. Meguro, K. Tuzimura, d-Pantolactone as a circular dichroism calibration, Anal. Biochem 67 (1975) 226–232.
[12] C.A. Rohl, R.L. Baldwin, Deciphering rules of helix stability in peptides, Methods Enzymol. 295 (1998) 1–26.
[13] K. Konno, M. Hisada, R. Fontana, C.C.B. Lorenzi, H. Naoki, Y. Itagaki, A. Miwa, N. Kawai, Y. Nakata, T. Yasuhara, J. Ruggiero Neto, W.F. Azevedo, M.S. Palma, T. Nakajima, Anoplin, a novel antimicrobial peptide from the venom of the solitary wasp *Anoplius samariensis*, Biochim. Biophys. Acta 1550 (2001) (2001) 70–80.
[14] S.F. Altschul, T.L. Madden, A.A. Schaffer, J. Zhang, Z. Zhang, W. Miller, D.J. Lipman, Gapped BLAST and PSI-BLAST: a new generation of protein database search programs, Nucleic Acids Res. 25 (1997) 3389–3402.
[15] G. Corzo, C. Bernard, H. Clement, E. Villegas, F. Bosmans, J. Tytgat, L.D. Possani, H. Darbon, A. Alagon, Insecticidal peptides from the theraposid spider *Brachypelma albiceps*: an NMR-based model of Ba2, Biochim. Biophys. Acta 1794 (2009) 1190–1196.
[16] H.M. Berman, J. Westbrook, Z. Feng, G. Gilliland, T.N. Bhat, H. Weissig, I.N. Shindyalov, P.E. Bourne, The protein data bank, Nucleic Acids Res. 28 (2000) 235–242.
[17] A. Sali, T.L. Blundell, Comparative protein modelling by satisfaction of spatial restraints, J. Mol. Biol. 234 (1993) 779–815.
[18] M.A. Marti-Renom, A.C. Stuart, A. Fiser, R. Sanchez, F. Melo, A. Sali, Comparative protein structure modeling of genes and genomes, Annu. Rev. Biophys. Biomol. Struct. 29 (2000) 291–325.
[19] A. Sali, J.P. Overington, Derivation of rules for comparative protein modeling from a database of protein structure alignments, Protein Sci. 3 (1994) 1582–1596.
[20] M.Y. Shen, A. Sali, Statistical potential for assessment and prediction of protein structures, Protein Sci. 15 (2006) 2507–2524.
[21] R.A. Laskowski, M.W. MacArthur, D.S. Moss, J.M. Thornton, PROCHECK: a program to check the stereochemical quality of protein structures, J. Appl. Crystallogr. 26 (1993) 283–291.
[22] W.L. Delano, The PyMOL Molecular Graphics System, DeLano Scientific, San Carlos, CA, USA, 2002. (Available from: http://www.pymol.org).
[23] D. Van Der Spoel, E. Lindahl, B. Hess, G. Groenhof, A.E. Mark, H.J. Berendsen, GROMACS: fast, flexible, and free, J. Comput. Chem. 26 (2005) 1701–1718.
[24] W.R.P. Scott, P.H. Hunenberger, I.G. Tironi, A.E. Mark, S.R. Billeter, J. Fennen, A.E. Torda, T. Huber, P. Kruger, W.F. van Gunsteren, The GROMOS biomolecular simulation program package, J. Phys. Chem. A 103 (1999) 3596–3607.
[25] H.J.C. Berendsen, J.P.M. Postma, W.F. van Gunsteren, J. Hermans, Interaction models for water in relation to proteins hydration, in: B. Pullman (Ed.), Intermolecular Forces, Reidel, Dordrecht, 1981, pp. 331–342.
[26] M. Fioroni, K. Burger, A.E. Mark, D. Roccatano, A model of 1,1,1,3,3,3-hexafluoropropan-2-ol for molecular dynamics simulations, J. Phys. Chem. B 105 (2001) 10967–10975.

[27] B. Hess, H. Bekker, H.J.C. Berendsen, J.G.E.M. Fraaije, LINCS: a linear constraint solver for molecular simulations, J. Comput. Chem. 18 (1997) 1463–1472.
[28] S. Miyamoto, P.A. Kollman, SETTLE: an analytical version of the SHAKE and RATTLE algorithm for rigid water models, J. Comput. Chem. 13 (1992) 952–962.
[29] H.J.C. Berendsen, J.P.M. Postma, W.F. van Gunsteren, A. DiNola, J.R. Haak, Molecular dynamics with coupling to an external bath, J. Chem. Phys. 81 (1984) 3684–3690.
[30] S. Chowdhuri, M.L. Tan, T. Ichiye, Dynamical properties of the soft sticky dipole–quadrupole–octupole water model: a molecular dynamics study, J. Chem. Phys. 125 (2006) 144513.
[31] U. Essmann, M.L. Perera, M.L. Berkowitz, T. Darden, H. Lee, L.G. Pedersen, A smooth particle mesh Ewald method, J. Chem. Phys. 103 (1995) 8577–8593.
[32] W. Humphrey, A. Dalke, W. Schulten, VMD — visual molecular dynamics, J. Mol. Graph. 14 (1996) 33–38.
[33] B.M. De Souza, A.V.R. Silva, V.M.F. Resende, H.A. Arcuri, M.P. Dos Santos Cabrera, J. Ruggiero Neto, M.S. Palma, Characterization of two novel polyfunctional mastoparan peptides from the venom of the social wasp *Polybia paulista*, Peptides 3 (2009) 1387–1395.
[34] W. Falk, R.H. Goodwin Jr., E.J. Leonard, Chemotaxis assay, J. Immunol. Methods 33 (1980) 239–247.
[35] J. Meletiadis, J.G.M. Meis, J.W. Mouton, V.P.E. Donnelly, Comparison of NCCLS and 3-(4,5-dimethyl-2-thiazyl)-2,5-diphenyl-2H tetrazolium bromide (MTT) methods of in vitro susceptibility testing of filamentous fungi and development of a new simplified method, J. Clin. Microbiol. 38 (2000) 2949–2954.
[36] M. Zimmermann, Ethical guidelines for investigations of experimental pain in conscious animals, Pain 16 (1983) 109–110.
[37] M. Chacur, I. Longo, G. Picolo, J.M. Gutierrez, B. Lomonte, J.L. Guerra, C.F. Teixeira, Y. Cury, Hyperalgesia induced by Asp49 and Lys49 phospholipases A_2 from *Bothrops asper* snake venom: pharmacological mediation and molecular determinants, Toxicon 41 (2003) 667–678.
[38] T. Horizoe, N. Nagakura, K. Chiba, H. Shirota, M. Shinoda, N. Kobayashi, H. Numata, Y. Okamoto, S. Kobayashi, ER-34122, a novel dual 5-lypoxygenase/cyclooxygenase inhibitor with potent anti-inflammatory activity in an arachidonic acid-induced ear inflammation model, Inflamm. Res. 47 (1998) 375–383.
[39] D.G. Kleinbaum, L.L. Kupper, K.E. Muller, A. NIzam, Analysis of Repeated Measures Data in Brooks/Cole Publishing Company — Applied Regression Analysis and Other Multivariable Methods, Brooks/Cole Publishing Co., 1998. 589–638.
[40] S.P. Ribeiro, M.A. Mendes, L.D. Santos, B.M. De Souza, M.R. Marques, W.F. Azevedo Jr., M.S. Palma, Structural and functional characterization of N-terminally blocked peptides isolated from the venom of the social wasp *Polybia paulista*, Peptides 25 (2004) 2069–2078.
[41] B.M. De Souza, M.A. Mendes, L.D. Santos, M.R. Marques, L.M.M. César, R.N.A. Almeida, F.C. Pagnocca, K. Konno, M.S. Palma, Structural and functional characterization of two novel peptide toxins isolated from the venom of the social wasp *Polybia paulista*, Peptides 26 (2005) 2157–2164.
[42] R. Patterson, L.C. Grammer, P.A. Greenberger, Patterson's Allergic Diseases. Asthma, 7th ed., Lippincott Williams & Wilkins, 2009.
[43] B.M. De Souza, M.S. Palma, Peptides from Hymenoptera venoms: biochemistry, pharmacology and potential applications in health and biotechnology, in: M.E. De Lima, A.M.C. Pimenta, M.F. Martin-Euclaire, R.B. Zingali (Eds.), Animal Toxins: The State of Art. Perspectives on Health and Biotechnology, UFMG Press, Belo Horizonte, Brazil, 2009, pp. 273–297.
[44] S.E. Blondelle, B. Forood, R.A. Houghten, E. Perez-Paya, Secondary structure induction in aqueous vs membrane-like environments, Biopolymers 42 (1997) 489–498.
[45] K.T. Fitzgerald, A.A. Flood, Hymenoptera stings, Clin. Tech. Small Anim. Pract. 21 (2006) 194–204.
[46] W. Berger, M.T. De Chandt, C.B. Cairns, Zileuton: clinical implications of 5-lipoxygenase inhibition in severe airway disease, Int. J. Clin. Pract. 61 (2007) 663–676.
[47] R. Patterson, L.C. Grammer, P.A. Greenberger, Patterson's Allergic Diseases. Asthma, 7th edition, Lippincott Williams & Wilkins, Wolters Kluwer, 2009.
[48] J.D. Levine, H.L. Field, A.I. Basbaum, Peptides and the primary afferent nociceptor, J. Neurosci. 13 (1993) 2273–2286.
[49] E.M. Zanchet, Y. Cury, Peripheral tackykinin and excitatory amino acid receptors mediate hyperalgesia induced by *Phoneutria nigriventer* venom, Eur. J. Pharmacol. 467 (2003) 111–118.
[50] S. Schenberg, F.A. Pereira-Lima, Phoneutria nigriventer venom, pharmacology and biochemistry of its components, in: W. Bucherl, E.E. Buckley (Eds.), Venomous Animals and Their Venoms, Academic Press, New York, NY, 1971, pp. 279–285.
[51] M. Chacur, G. Picolo, J.M. Gutiérrez, C.F.P. Teixeira, Y. Cury, Pharmacological modulation of hyperalgesia induced by *Bothrops asper* (terciopelo) snake venom, Toxicon 39 (2001) 1173–1181.